

Combined Effect of Diaphragm and Oxidizer Swirl on Regression Rate in Hybrid Rocket Motors

C. Palani Kumar and Amit Kumar*

Indian Institute of Technology Madras, Chennai-600 036, India

**E-mail: amitk@ae.iitm.ac.in*

ABSTRACT

The present numerical work investigates the effect of a combination of two known regression rate enhancement techniques, namely diaphragm located in the port and swirling oxidizer flow at the inlet. Diaphragm enhances regression rate by heat transfer enhancement due to recirculation zone whereas swirling flow enhances regression rate by enhancement in radial diffusive transport. The use of diaphragm in combination with swirl was found to be more effective in enhancing regression rate compared with the individual enhancements by the two techniques. However, the net enhancement in regression rate using combined techniques was less than the arithmetic sum of enhancement from two individual techniques. Interestingly, the characteristic exhaust velocity C^* is enhanced only if diaphragms are sufficiently tall.

Keywords: Hybrid rocket, regression rate, diaphragm, swirling flow, numerical study

1. INTRODUCTION

One of the most significant design parameters in hybrid rocket motor is the regression rate, defined as the rate at which the solid fuel regresses normal to the surface. Decades of research has contributed greatly towards understanding of fundamental operation of hybrid rocket motors. A theoretical explanation of processes inside the hybrid motor was first proposed by Marxman¹, where a regression rate model based on the turbulent boundary layer theory for heat transfer was described. In a hybrid rocket motor, the fuel and the oxidizer react forming a diffusion flame front inside the combustion chamber. A part of the heat released in the reaction is used in the pyrolysis of solid fuel. Therefore, the attempts to enhance regression rate are primarily focused on increasing the heat feed back to the solid fuel. Some of the methods for increasing the regression rate of the solid fuel include addition of energetic additives to solid fuel grain², introduction of swirl in the oxidizer flow^{3,4} or provision of turbulence generators⁵ or diaphragms in the port^{6,7}.

Extensive numerical studies had already been performed to assess the effect of diaphragms⁸ and inlet swirl⁹ on the regression rate and performance of hybrid rocket motor. However, the effect of these two techniques in combination has not yet been investigated. In the present work reported here, a systematic parametric study is performed to investigate numerically the effect of diaphragms and swirling inlet oxidizer flow in combination.

2. NUMERICAL MODEL

The numerical model used in the present study is explained in detail in recent works by the authors^{8,9}. Hence, only the aspects of model relevant to this study are briefly discussed here.

2.1 Geometrical Configuration and Computational Domain

A laboratory scale motor with a single port grain is chosen for carrying out simulations as this configuration is amenable to experiments. Figure 1 (a) presents the schematic of a generic single port hybrid rocket motor with the following grain dimensions; the outer diameter - D_o , the initial inner diameter - D_i , the port diameter at an arbitrary instant of burning of grain - D , the length of the motor - L , the nozzle throat diameter - D_t , and the nozzle exit diameter - D_e .

The computational domain is assumed to be axially symmetric for numerical simplicity. Hence the numerical model is presented in 2-D axi-symmetric configuration. In Fig. 1 (a) the region shaded by inclined stripes represents the computational domain which comprises of the grain port at an arbitrary instant of burning and the nozzle. The grain port diameter (D) is taken as 30 mm and the port length (L) is 150 mm. The nozzle throat diameter (D_t) is 14 mm and nozzle exit diameter (D_e) is 30 mm. Mesh is constructed in the computation domain with quadrilateral cells. Fine mesh is used near boundaries is shown in Fig. 1 (b) to resolve the gradients accurately. Grid independence study was conducted by reducing the size of smallest grid by an order till the difference between predicted average regression rates for two finest meshes was within 5%. The grid size used in the computation domain reported in the present work is 176 x 111.

2.2 Governing Equations

The transport processes occurring in a hybrid rocket combustion chamber are described adequately by the basic flow equations of continuity, momentum, energy and species. The turbulence in the flow is modeled using Menter's two-equation

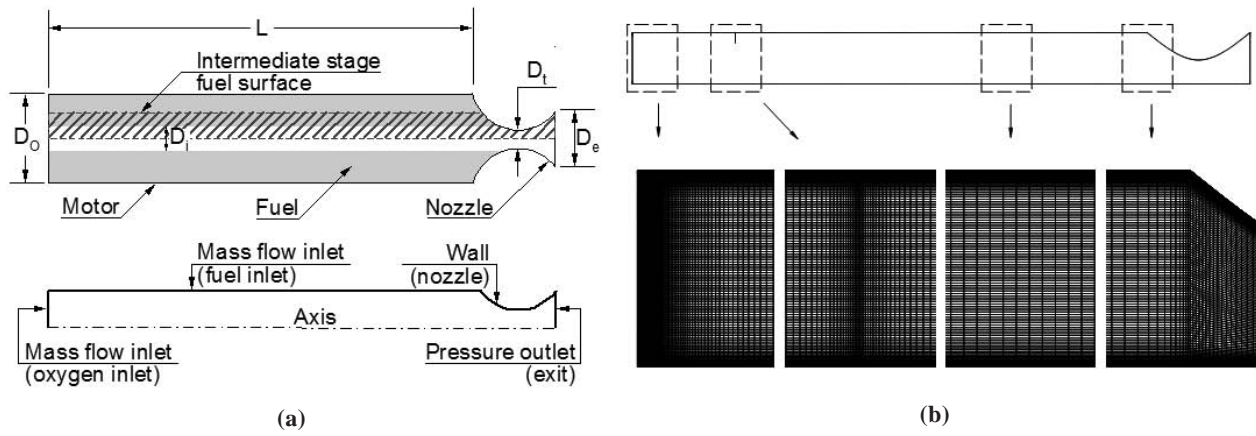


Figure 1 (a) Schematic diagram of a hybrid rocket motor with boundary types used in computation and (b) Grid used in the computation (with a diaphragm)

SST $k-\omega$ model¹⁰. The governing equations in 2-D cylindrical co-ordinates are described^{8,9}.

2.3 Gas Phase and Solid Phase Chemistry Models

A global one step chemistry is used to model the oxidation of butadiene (monomer of HTPB) to final products CO_2 and H_2O . The gas phase kinetics is adopted from work of Cheng¹¹, *et al.* Although detailed chemistry is desired for accurate predictions, such a reaction mechanism and related kinetics are not yet available in the literature. Nevertheless, the thermodynamic effect of product disassociation is incorporated by tuning the heat of combustion to match the temperature with one obtained accounting for product dissociation at thermodynamic equilibrium¹². The solid fuel (HTPB) pyrolysis is modeled¹³ by a zeroth order Arrhenius equation.

2.4 Boundary Conditions

The boundary types are illustrated in Fig. 1 (a). The boundary condition at gas-fuel interface is implemented by applying mass and energy balance. The energy balance at the interface is given below^{8,9}.

$$\lambda_{eff} \left(\frac{\partial T}{\partial y} \right)_g - \lambda_s \left(\frac{\partial T}{\partial y} \right)_s + \rho_s r_b (H_p) = 0 \quad (1)$$

The terms on the left hand side represent the heat convected from reaction zone and conducted to the fuel surface ($q_{\text{convection}}$), heat conduction into the solid fuel ($q_{\text{conduction-loss}}$) and the heat of solid fuel pyrolysis ($q_{\text{pyrolysis}}$).

The oxidizer mass flux at the inlet is set to 132 $\text{kg}/(\text{m}^2 \cdot \text{s})$ for both swirling and non-swirling flow simulations. The inlet swirl is quantified by a non-dimensional parameter called swirl number, S_w . S_w is defined¹⁴ as the ratio of the axial flux of angular momentum to the axial flux of axial momentum, non-dimensionalised by inlet radius.

$$S_w = \frac{\int \rho v_x v_z r^2 dr}{R_0 \int \rho v_x^2 r dr} \quad (2)$$

The profiles for axial and swirl velocities¹⁴ are also prescribed at the oxidizer inlet. The nozzle wall is defined as an adiabatic wall and ambient pressure is specified at the outlet.

2.5 Numerical Method of Solution

The governing equations and the models for solid and gas phases along with the boundary conditions discussed above are solved numerically using a pressure based, double precision, unsteady solver¹⁵. Unsteady solver is used to predict any transient phenomena like vortex shedding that might occur in the combustion chamber. Second order upwind scheme is used for spatial discretisation of the convective terms whereas second order central scheme is used for all other terms in the transport equations. The second order implicit formulation is used for temporal discretisation.

The discretised governing equations are iterated with the time step of 0.0002 s and with 50 iterations for every time step. The converged solution is typically attained in about 1000 time steps. The model was validated⁸ for the prediction of regression rate against the experimental results¹⁶. The ability of the numerical model to predict swirl flow in a pipe was also demonstrated⁹ against experimental results¹⁷.

3. RESULTS AND DISCUSSIONS

The following methodology is adopted in the present work to investigate the effect of diaphragm and swirling oxidizer inlet flow in combination.

First, the base motor (one without any enhancement technique) is discussed. This is followed by a brief discussion on a motor with any one regression rate enhancement technique (diaphragm or swirl). With the basic understanding obtained from the above studies simulations with a combination of diaphragm and swirl were carried out in two sets. In the first set, a representative inlet swirl was chosen (inlet $S_w = 1$) and the diaphragm height is varied from 1 mm to 7 mm. In the second set of simulations a representative diaphragm (7 mm tall) was chosen and the inlet S_w is varied from 0 to 2.5. The results obtained are discussed below.

3.1 Base Case Motor

Figure 2 presents the components of heat flux at the interface Eqn. (1), local regression rate and fuel surface temperature along the axial length of the fuel grain. It can be noticed that the heat flux component $q_{\text{convection}}$ is the only source of heat feedback to the fuel surface. Thus the regression rate

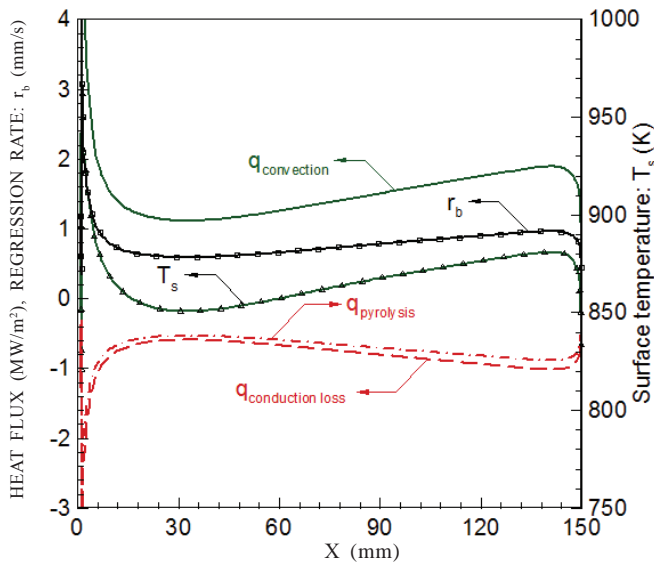


Figure 2. Components of heat flux, local regression rate and surface temperature of solid fuel, along the axial length of the hybrid rocket motor for base case.

and the surface temperature follow the trend of $q_{convection}$.

The heat flux components and the local regression rate decrease along the axial length of the grain up to a certain distance (here, about 30 mm) and then increase. This is caused by two competing phenomena occurring in the combustion chamber. Near the head end (< 5 mm) the flame is very close to the fuel surface and the regression rate is high. Downstream, the flame is pushed away from the fuel surface due to fresh fuel addition. Hence, the heat transfer and thereby the regression rate decreases. However, due to progressive addition of fuel vapour, the local mass flux increases along the axial length. This increases heat transfer and consequently the regression rate. The effect of flame being pushed away is dominant near the head end ($X < 30$ mm) and the effect of increasing mass flux is dominant downstream ($X > 30$ mm).

3.2 Effect of Individual Regression Rate Enhancement Techniques

The effect of diaphragms on regression rate is explored⁸. To describe the effects of diaphragm here we only discuss a single diaphragm of height 4 mm located at 0.25 L (37.5 mm) from the head end of the base motor.

Figure 3 shows the convective heat flux and local regression rate for representative cases to demonstrate the effect of a single diaphragm or inlet swirling oxidizer flow. For the case with diaphragm it can be noted that the heat feedback reduces and thus regression rate decreases considerably upstream of the diaphragm. This is because the diaphragm diverts the flow (and the flame) away from the fuel surface there by reducing the heat transfer upstream of diaphragm. Downstream of the diaphragm, the regression rate recovers and increases sharply over a short distance. This is because of a recirculation zone formed downstream of the diaphragm that entrains the hot gases from the reaction zone towards the fuel surface. Therefore, the local regression rate is enhanced attaining a peak value at the tip of the recirculation zone (here, about 60

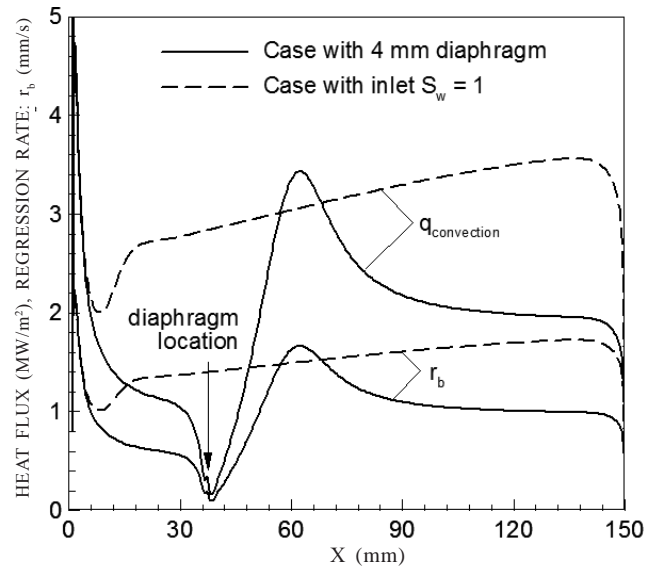


Figure 3. Effect of a single diaphragm located at $x = 37.5$ mm or swirling oxidizer flow at inlet on convective heat flux along the axial length of the hybrid rocket motor

mm). Further downstream of the recirculation zone, the hot products are progressively cooled by addition of fuel vapour and consequently the regression rate decreases.

For the case with swirl (inlet $S_w = 1$) it can be noted that the local regression rate follows the decreasing-increasing trend similar to the base case. However, the local minimum in the regression rate attained is higher and much closer to the head end. The presence of swirl velocity in the flow results in higher velocity magnitude in the combustion chamber. This enhances the radial heat and momentum transport in the combustion chamber. Thus the heat flux components at the interface are enhanced thereby enhancing the regression rate.

3.3 Effect of Regression Rate Enhancement Techniques in Combination

Now we look at the combined effect of the two enhancement techniques to the base motor. Figure 4 illustrates the effect of diaphragm height on the local regression rate for simulations in the presence and absence of inlet swirl. One may note that in both the cases (i.e. with or without swirl in the flow), the local regression rate increases significantly downstream of the diaphragm, attains a local peak value and then decreases. However, in the presence of swirling flow the peak in the local regression rate increases and location at which the peak value occurs shifts closer to the diaphragm. The diaphragm in the port diverts the flow towards the core. However, the enhanced radial transport associated with swirling flow expands the flow steeply downstream of the diaphragm resulting in a smaller recirculation zone (inferred from peak regression rate location which is also the tip of the recirculation zone). One can also note that the regression rate attained with both the techniques in combination is higher than the regression rate attained with individual enhancement techniques indicating that both diaphragm and swirl complement each other in regression rate enhancement. However, it is also to be noted that cumulative enhancement (2.00 mm/s $- 0.68$ mm/s $= 1.32$ mm/s) over

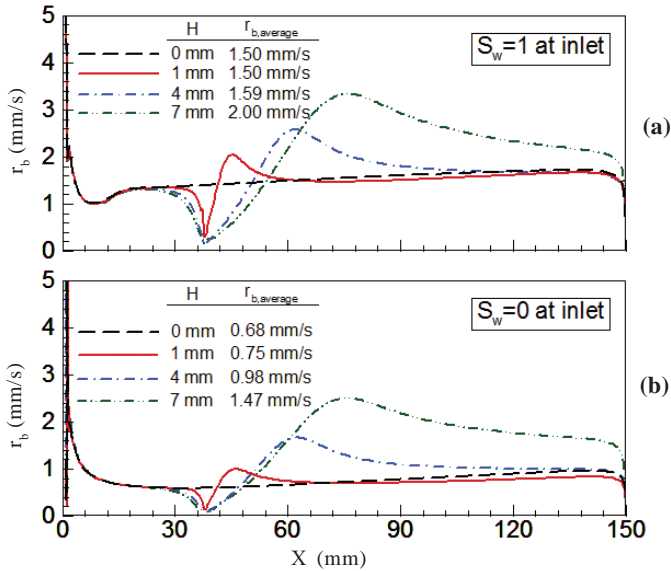


Figure 4. Effect of diaphragm height on the local regression rate along the axial length of the fuel grain for simulations in the presence (a) and absence (b) of swirling oxidizer flow at the inlet.

the base motor value (0.68 mm/s) is less than the sum of the enhancements with the individual techniques (0.82 mm/s enhancement for swirl and 0.79 mm/s enhancement for diaphragm). This is because while the diaphragm enhances regression rate by forming recirculation zone behind the diaphragm, the flame downstream of diaphragm is pushed farther from the fuel surface. Similarly the swirl in the flow increases velocity magnitude and radial transport, however, the centrifugal force causes the low density flame to move towards the axis away from fuel surface. Thus the negative effects of the two techniques also complement each other.

Figure 5 presents variation of average regression rate, overall O/F ratio and characteristic exhaust velocity C^* for the case with a single diaphragm. The solid lines show the variation of parameters in the presence of swirling flow and the dashed lines show those in the absence of swirling flow in the combustion chamber. The average regression rate and C^* for any diaphragm height is higher in the presence of swirling flow compared to that in the absence of swirling flow. The average regression rate increases with diaphragm height in the presence or absence of swirling inlet oxidizer flow. However, for the case with swirling flow, the enhancement in average regression rate is not significant for shorter diaphragms (here, < 4 mm). In both cases C^* is seen to show a decreasing-increasing trend with increase in diaphragm height. The diaphragm increases mixing of reactants in the recirculation zone at the same time it also holds the flame farther from the fuel surface. This leads to progressive addition of un-reacted fuel vapor between reaction zone and fuel surface. While the former effect (mixing) increases C^* the later effect (unreacted fuel vapor) decreases C^* . For short diaphragms addition of un-reacted fuel vapor is dominant causing a reduction in C^* , whereas for tall diaphragms (≥ 4 mm), mixing in the recirculation zone becomes dominant due to larger recirculation zones resulting in enhanced C^* . It is to be noted that the motor considered in the present study contains

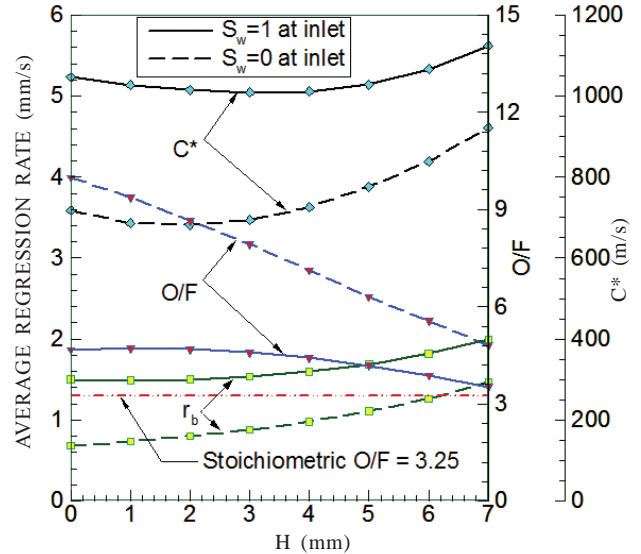


Figure 5. Effect of diaphragm height on performance parameters of the motor with inlet $S_w = 1$ (solid lines) and inlet $S_w = 0$ (dashed lines).

a short grain with L/D ratio of 5. One can note that the O/F values are far from the stoichiometric value of 3.25 indicating fuel lean operation. Thus all the oxidizer is not consumed at the end of combustion chamber. With the increasing regression rate in the presence of taller diaphragms the O/F ratio is seen to decrease.

The swirl number was kept constant in the simulations discussed in Fig. 5. Next we look at effect of inlet S_w on the regression rate, overall O/F ratio and C^* in the presence or absence of a diaphragm of fixed height (here, 7 mm) as shown in Fig. 6. Both in the presence and absence of a diaphragm, the average regression rate is seen to increase monotonically with increase in inlet S_w . This is because, larger inlet S_w results in larger velocity magnitude and thus increased radial transport. This increases the heat flux at the interface and as a consequence the regression rate increases. With increased regression rate for the same inlet oxidizer flow, the O/F ratio decreases. Increase in swirl also enhances C^* owing to increased radial mixing⁹.

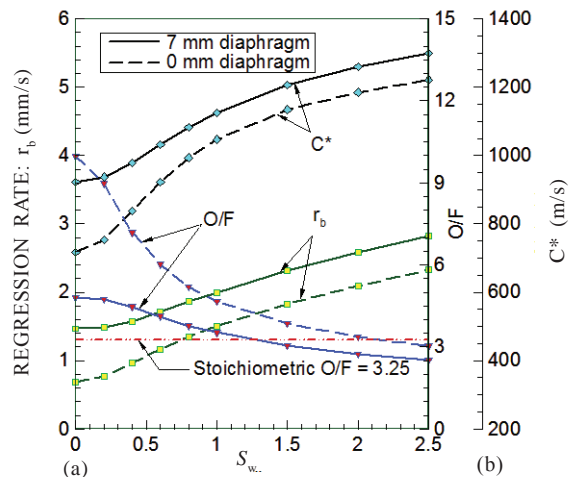


Figure 6. Effect of inlet S_w on performance parameters of the motor in the presence (solid lines) and the absence (dashed lines) of a 7 mm diaphragm located at 0.25 L from the head end.

The average regression rate is higher in the presence of diaphragm than that in the absence of diaphragm at any inlet S_w . Consequently the O/F ratio is always lower in the presence of diaphragm compared to no diaphragm case. One can note that the stoichiometric O/F is achievable here with this short motor for $S_w > 2$. Strong recirculation zone behind the diaphragm promotes mixing gases in the recirculation zone thereby result in higher C^* compared to no diaphragm cases at all inlet S_w .

4. CONCLUSIONS

A numerical study was carried out on single port laboratory scale hybrid rocket motor to understand the combined effect of diaphragm and swirl in flow in enhancing regression rate and the performance of the rocket motor. A systematic study was first carried out to assess the effect of a single diaphragm of various heights in the presence and absence of swirling oxidizer flow at the inlet. Further study was carried out to assess the effect of inlet swirl strength (characterized by swirl number, S_w) in the presence and absence of a diaphragm. Based on the above discussions, the following conclusions may be drawn.

The local regression rate along the fuel grain length in a hybrid rocket motor is seen to follow the heat transferred from the gas phase to the fuel surface. Presence of diaphragm in the port causes a recirculation zone downstream of diaphragm. This recirculation zone transports hot gases from the flame closer to the fuel surface and enhances heat feedback to the fuel. Mixing in the recirculation zone also promotes C^* . Swirling oxidizer flow at the inlet contributes an additional swirl component to the velocity thereby increasing velocity magnitude in the combustion chamber. Thus the radial gradients are higher and the radial diffusive transport and mixing of gases are enhanced.

The positive effect of both diaphragm and swirl (enhanced heat transfer at the fuel surface) complement each other. Therefore, the combination of the two techniques is seen to enhance the regression rate better compared to the individual contribution of the techniques. For a given inlet S_w , the average regression rate is enhanced with increase in diaphragm height. The enhanced mixing in the recirculation zone promotes C^* enhancement and is dominant for taller diaphragms. The flame that is held farther from fuel surface by diaphragm demotes C^* enhancement and is dominant for shorter diaphragms. Hence C^* has a decreasing-increasing trend with increase in diaphragm height. On the other hand for a given diaphragm height, the average regression rate as well as the C^* are enhanced with increase in inlet S_w . The negative effect of both diaphragm and swirl (flame held farther from the fuel surface) also complement each other. Therefore, the combined enhancement of regression rate by diaphragm and swirl in combination is lesser than the arithmetic sum of the regression rate enhancement contributed by diaphragm and swirl individually.

REFERENCES

- Marxman, G. A. Combustion in turbulent boundary layer on a vaporizing surface. *In the 10th International Symposium on Combustion*, Combustion Inst., Pittsburgh, PA, 1965, pp.1337-1349.
- George, P. & Krishnan, S. Fuel regression rate in hydroxyl-terminated polybutadiene/gaseous oxygen hybrid rocket motors. *J. Prop. Power*, 2001, **17**(1), 35-42.
- Knuth, W.H.; Chiaverini, M.J.; Sauer, A. & Gramer, D.J. Solid-fuel regression rate behavior of vortex hybrid rocket engines. *J. Prop. Power*, 2002, **18**(3), 600-609.
- Lee, C.; Na, Y. & Lee, G. The enhancement of regression rate of hybrid rocket fuel by helical grain configuration and swirl flow. *In the Proceedings of 41st AIAA/ASME/SAE/ASEE Joint Propulsion Conference & Exhibit*, Tucson, AZ, 2005. AIAA Paper 2005-3906.
- Altman, D. & Holzman, A. Overview and history of hybrid rocket propulsion. *Fundamentals of Hybrid Rocket Combustion and Propulsion*, Edited by, Chiaverini M.J. & Kuo, K.K. **218**, *In the Progress in Aeronautics and Astronautics*, AIAA, Reston, Virginia, 2007, pp. 1-36.
- Matthias Grosse. Effect of a diaphragm on performance and fuel regression of a laboratory scale hybrid rocket motor using nitrous oxide and paraffin. *In the Proceedings of 45th AIAA/ASME/SAE/ASEE Joint Propulsion Conference & Exhibit*, Denver, CO, 2009. AIAA Paper 2009-5113.
- Bellomo, N; Lazzarin, M.; Barato, F. & Grosse, M. Numerical investigation of the effect of diaphragm on the performance of a hybrid rocket motor. *In the Proceedings of 46th AIAA/ASME/SAE/ASEE Joint Propulsion Conference & Exhibit*, Nashville, TN, 2010. AIAA Paper 2010-7033.
- Kumar, C.P. & Kumar. A. Numerical investigation on the effect of diaphragms on regression rate in hybrid rocket motors. *J. Propulsion Power*, 2012, **29**(3), 559-572.
- Kumar. C.P. & Kumar, A. Effect of swirl on the regression rate in hybrid rocket motors. *Aerospace Sci. Techno.*, 2013, **29**(1), 92-99.
- Menter, F.R. Two equation Eddy-viscosity turbulence models for engineering applications. *AIAA Journal*, 1994, **32**(8), 1598-1605.
- Cheng, G.C.; Farmer, R.C.; Jones H.S. & McFarlane, J.S. Numerical simulation of internal ballistics of a hybrid rocket motor. *In Proceedings of 32nd Aerospace Sciences Meeting and Exhibit*, AIAA Paper 1994-0554, Reno, NV, 1994.
- Gordon, S. & McBride, B.J. Computer program for calculation of complex chemical equilibrium compositions and applications. NASA Reference Publication 1311, 1996.
- Ramakrishna, P.A.; Paul P.J. & Mukunda, H.S. Sandwich propellant combustion: Modeling and experimental comparison. *In the Proceedings of the Combustion Institute*, 29, The Combustion Institute, 2002, **29**(2), 2963-2973.
- Jiang, X; Siamas, G.A. & Wrobel, L.C. Analytical equilibrium swirling inflow conditions for computational fluid dynamics. Technical notes, *AIAA Journal*, 2008, **46**(4), 1015-1019.
- ANSYS-Fluent Software. Version No. 6.3.26, 2006.
- Kuo, K.K; Lu, Y-C; Chiaverini, M.J; Johnson, D.K; Serin, N; Risha, G.A; Merkle, C.L. & Venkateshwaran, S. Fundamental phenomena on fuel decomposition and

boundary layer combustion processes with applications to hybrid rocket motors. Semi-Annual Progress Report, NASA-CR-201843, June 1996.

17. Steenbergen, W. & Voskamp, J. The rate of decay of swirl in turbulent pipe flow. *Flow Measurement Instrumen.*, 1998, **9**(2), 67-78.

CONTRIBUTORS



Mr C. Palani Kumar obtained his BE (Mechanical Engineering) from Kumaraguru College of Technology, Coimbatore in 2004. He is currently pursuing his PhD (Aerospace Engineering) in IIT Madras. His research and work experience includes hybrid rockets, computational combustion and propulsion.



Dr Amit Kumar obtained his PhD (Mechanical & Aerospace) from Case Western Reserve University, Cleveland, Ohio in 2004. He is currently working as Associate professor in the department of Aerospace Engineering, IIT Madras. His research work and area of expertise includes hybrid propulsion, computational combustion, fire safety (microgravity to terrestrial environments), electric propulsion and DDT.